Direct Visualization of Dynamic Protein-DNA Interactions with a Dedicated Atomic Force Microscope

S. John T. van Noort,* Kees O. van der Werf,* Andre P. M. Eker,# Claire Wyman,# Bart G. de Grooth,* Niek F. van Hulst,* and Jan Greve*

*Department of Applied Physics, University of Twente, 7500 AE Enschede, and #Department of Cell Biology and Genetics, Medical Genetics Centre, Erasmus University, 3000 DR Rotterdam, The Netherlands

ABSTRACT Photolyase DNA interactions and the annealing of restriction fragment ends are directly visualized with the atomic force microscope (AFM). To be able to interact with proteins, DNA must be loosely bound to the surface. When $MgCl_2$ is used to immobilize DNA to mica, DNA is attached to the surface at distinct sites. The pieces of DNA in between are free to move over the surface and are available for protein interaction. After implementation of a number of instrumental improvements, the molecules can be visualized routinely, under physiological conditions and with molecular resolution. Images are acquired reproducibly without visible damage for at least 30 min, at a scan rate of 2×2 μm^2/min and a root mean square noise of less than 0.2 nm. Nonspecific photolyase DNA complexes were visualized, showing association, dissociation, and movement of photolyase over the DNA. The latter result suggests a sliding mechanism by which photolyase can scan DNA for damaged sites. The experiments illustrate the potential that AFM presents for modern molecular biology.

INTRODUCTION

With the introduction of atomic force microscopy (AFM), imaging of biological samples under physiological conditions with nanometer resolution became possible, and the use of AFM to study processes between individual active molecules became a challenging goal (Hansma, 1995; Lal and John, 1994). However, because of the many difficulties that arise during such experiments (Thomson et al., 1996), only a few studies visualizing single molecular interactions have been reported so far.

In one of the first papers describing direct measurement of single molecular activity with AFM, height variations on lysozyme were observed and attributed to the enzyme's activity (Radmacher et al., 1994). Ligand-receptor interactions between various functional molecules have been measured in force-distance mode (Florin et al., 1994), and only very recently Kasas et al. (1997) have impressively used the imaging possibility of AFM to visualize the process of RNA transcription. The mobility of the DNA molecules, which was necessary for RNA polymerase activity, however, prevented the DNA from being imaged clearly, complicating the interpretation of the measurements.

To reproducibly achieve good quality AFM data in physiological conditions, high demands are made on the AFM system, the imaging parameters, and the sample preparation. In this paper both AFM parameters that result in reproducible images and the reaction conditions allowing imaging of interactions between single photolyase molecules and DNA are discussed. The stability demands and improvements, which have been implemented in our AFM set-up, are described. The temporal resolution was maximized for commercially available cantilevers, without sacrificing image quality. In this way, time series of images were obtained, showing many different intra- and intermolecular events.

AFM imaging of DNA

Because of its essential role in biology DNA has been studied extensively by AFM (Hansma et al., 1996). Studies of protein DNA complexes in air have provided information about binding sites and stoichiometry of the proteins and ligand-induced bending of DNA (Erie et al., 1994; Wyman et al., 1995, 1997). Even the double-helix structure has been resolved with AFM when the DNA was imaged under propanol or butanol. However, most importantly, AFM is unique in providing the possibility of studying biochemical processes at a single molecule level, under physiological conditions, as demonstrated in the study of RNA polymerase (Kasas et al., 1997).

As AFM is a surface technique, the reactions have to proceed on a surface. In fact, a paradoxical problem has to be overcome. To be able to image DNA reproducibly and with high resolution, it is necessary that DNA is attached to the surface. Otherwise the DNA molecules would be swept away when the tip taps on the molecules, and the image would be severely distorted. However, to be available for interaction with other molecules, DNA must be free from the surface to avoid steric hindrance that might affect the reactions. Thus DNA should be immobilized just firmly enough to allow both imaging with AFM and interaction with proteins.

Because of its flatness, mica is the most commonly used substrate for DNA imaging (Hansma and Laney, 1996).

Received for publication 3 December 1997 and in final form 24 February 1998.

Address reprint requests to Dr. John van Noort, Department of Applied Physics, University of Twente, P.O. Box 217, 7500 AE Enschede, the Nehterlands. Tel.: 31-534-894002; Fax: 31-534-891105; E-mail: s.j.t.vannoort@tn.utwente.nl.

0006-3495/98/06/2840/10 $2.00

DNA, with its negatively charged phosphate backbone, is bound to the negatively charged mica surface by the addition of bivalent cations, which function as an electrostatic bridge. In addition to this effect, ions in the buffer will shield electrostatic charges and thus lower the repulsion between DNA and mica. A compromise between firm and loose immobilization has been achieved by optimizing the concentration and type of mono- and bivalent cations (Guthold et al., 1994). In this paper we will show that DNA immobilized on mica in a buffer containing 1 mM $MgCl_2$ and 1 mM NaCl is only partially bound to the mica surface at specific binding points; the loose parts move over the surface and are free to interact with proteins.

Nonspecific protein-DNA interactions

To show the ability to study protein-DNA interactions with AFM, formation of nonspecific complexes of dsDNA with photolyase was monitored. Photolyase is a well-studied enzyme responsible for the removal of thymine dimers in DNA (Sancar, 1994; Park et al., 1995; Hearst, 1995). The crystal structure was resolved (Park et al., 1995; Tamada et al., 1997), and structural features have been related to results from photochemistry. Although the reaction has been extensively described biochemically, AFM can contribute to a better understanding of the dynamic aspects of the reaction, such as the process of locating the damaged site.

Proteins that bind to specific sites on DNA can find these sites by two general mechanisms (Berg et al., 1981). Facilitated one-dimensional diffusion involves, first, binding nonspecifically to DNA, then moving along the DNA in search of specific sites (Dowd and Lloyd, 1990). Alternatively, proteins can locate specific sites on DNA by simple diffusion from solution. Although these dynamic protein-DNA interactions have not been demonstrated directly, in some cases biochemical evidence favors one mechanism over the other.

For instance, T4 endonuclease V, a repair enzyme that incises one strand at the site of pyrimidine dimers, is believed to slide along DNA in search of damaged sites. The mechanism photolyase uses to locate damaged sites is not known yet. In this paper we use AFM to directly visualize the interaction between photolyase and DNA. Although we studied only nonspecific interactions, we will show that AFM can be used to directly determine whether proteins are able to slide along DNA.

MATERIALS AND METHODS

Sample preparation

Freshly cleaved mica discs (Ted Pella) were used as a substrate for immobilizing DNA. Undamaged 500-bp dsDNA (Gensura), obtained by digesting plasmid DNA with *Eco*RI, was diluted to a final concentration of 2 ng/μl in a buffer containing 4 mM HEPES, 1 mM NaCl, and 1 mM $MgCl_2$ (pH 6.5). The buffers were made in MilliQ-filtered, deionized water. Photolyase, obtained from *Anacystis nidulans* (Eker et al., 1990; Tamada et al., 1997), was added to a final concentration of 0.12 ng/μl in the reaction buffer.

After 10 min at room temperature, 5 μl of the reaction mixture was deposited on mica. Directly after deposition, the AFM was mounted over the sample, and after a minute the liquid cell of the AFM was thoroughly rinsed with HEPES buffer, without DNA and photolyase. During sample preparation, mounting of the AFM and measurements, biomolecules remain in buffer and are never dehydrated, keeping them functional.

AFM set-up

A home-built stand-alone atomic force microscope (Van der Werf et al., 1993) was modified for the measurements reported. Triangular Si_3Ni_4 cantilevers with a spring constant of 0.5 N/m were purchased from Park Scientific instruments (Sunnyvale, CA). For our experiments, it was not necessary to use electron beam-deposited supertips to get reproducible images, as suggested in the literature (Kasas et al., 1997). Images with a scan area of 2×2 μm^2, 512×512 pixels, were continuously acquired in tapping mode, at a frequency of 25–35 kHz, a free amplitude of 6 nm, a peak-peak amplitude set-point of 5 nm, and a frame rate of 1 image/min.

Time series of images were processed using Interactive Data Language (RSI) in a self-written software package. Standard image processing consisted of line subtraction by fitting of a two-order polynomial to each line in the image. Residual lateral drift in the images was corrected for by cross-correlation of successive images.

Imaging parameters

For stable imaging of the loosely bound DNA with high resolution, it is essential to keep destructive tip-sample interaction forces to a minimum. AFM in liquid has the advantage that capillary forces, which are responsible for large tip adhesion at ambient conditions, are absent. However, it was only after the introduction of tapping mode AFM in liquid (Putman et al., 1994; Hansma et al., 1994) that weak biological samples could be imaged reliably without considerable damage, because of the reduction of destructive lateral forces between the tip and the sample.

Although lateral forces are absent in tapping mode, normal forces can have a great impact on the sample stability and image quality. In general, the smaller the amplitude, the less energy is available for damaging work during the impact on the sample. Keeping the tapping amplitude small is advantageous for keeping the sample stable for a second reason. In tapping mode in liquid, the cantilever is driven by acoustic waves in the liquid (Putman et al., 1994). The acoustic vibrations not only excite the cantilever, they will also shake up loose parts of the sample. In addition to tip-induced damage, sonication will remove loose parts from the surface, which is in conflict with the need to keep DNA bound to the surface. Thus it is favorable to keep vibrations in the liquid cell to a minimum.

After each impact of the tip on the sample, enough oscillatory energy must remain available in the cantilever to overcome tip-sample adhesion (Van Noort et al., 1997). Nonspecific adhesion forces can range up to a few hundred piconewtons, which would require a peak-peak amplitude of at least 2 nm when a cantilever with a spring constant of 0.5 N/m is used. Furthermore, for a linear amplitude response to a change in topography, which is required for the feedback loop, the linear regime of the amplitude versus distance should be large enough to overcome steep height variations when the tip is scanned over the surface at high velocities. In our experiments, a free peak-peak oscillation amplitude of 6 nm proved to be the best choice for good quality images.

In addition to a small driving amplitude, the damping of the oscillation should be minimal, to prevent damage of the sample (Han and Lindsay, 1996). We used an amplitude set point of 5 nm, corresponding to a 15% reduction of the free oscillation amplitude.

RESULTS

Improvements in the AFM set-up

Increase of deflection sensitivity

For an accurate measurement of the topography, it is necessary to be able to detect all topography-induced amplitude variations. The sensitivity of the deflection detection scheme, and thus the amplitude detection, is limited for two reasons. First, the RMS noise in the detection electronics of the whole system is generally ~0.5 mV. Second, and more fundamentally, the thermal movement of the cantilever introduces extra deflection, independent of the topography of the surface. By matching electronic noise with thermal noise of the cantilever, a lower limit for deflection sensitivity can be obtained. Thermal noise can be described by the equipartition theorem, demanding $0.5\ kT = 0.5\ Kx^2$ (Butt and Jaschke, 1995), where k is Boltzmann's constant, T is the absolute temperature, K is the spring constant, and x^2 is the mean square deflection of the cantilever. For $T = 293$ K and $K = 0.5$ N/m, sqrt(x^2) becomes 0.09 nm. Thus, to reach the thermal noise limit, the deflection sensitivity should be at least 5.6 mV/nm. To qualify for this requirement, laser power was increased to ~2 mW, which results in an optical power of 0.2 mW on the quadrant detector, because of reflection losses at the surfaces in the light path. The resulting deflection sensitivity was 9 mV/nm, limited by the range of the detector, making thermal noise of the cantilever the dominant noise source.

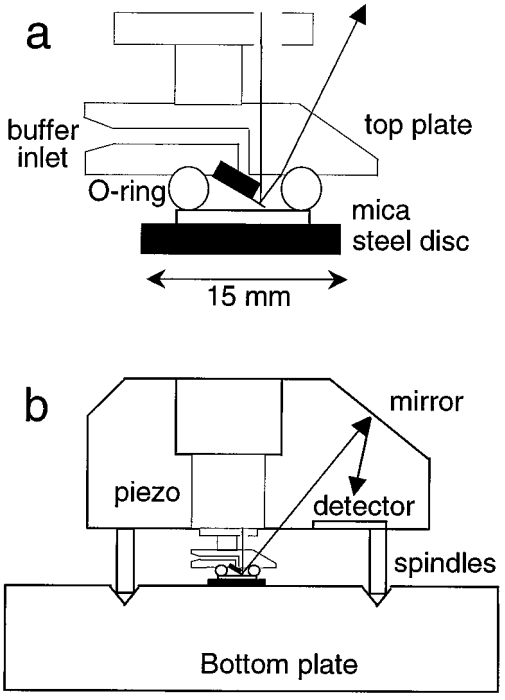

FIGURE 1 (*a*) Schematic drawing of the liquid cell, which is attached to the piezo scanner. In this set-up the Plexiglas top plate, on which the cantilever is mounted, scans over the mica substrate. (*b*) Schematic drawing of the whole stand-alone atomic force microscope. The microscope head is put on three spindles on the bottom plate. The scanner, the laser diode, and the detection electronics are built inside the housing.

Modifications in the AFM design

During long-term experiments, the buffer in an open liquid cell is prone to evaporation. The change in liquid volume can have a dramatic effect on the stability of the AFM measurement. As the cantilever is excited by acoustic waves in the liquid cell, a peak in the frequency spectrum points at an acoustic mode in the liquid cell, which is excited very efficiently, depending on the dimensions of the liquid cell (Putman et al., 1994; Schäfer et al., 1996). The tapping frequency is generally chosen on a peak in the frequency spectrum of the cantilever deflection. Even a small loss in liquid volume causes a change in the acoustic modes in the cell, resulting in less efficient excitation of the cantilever. These unanticipated changes in tapping amplitude, not originating from the topography of the sample and thus resulting in severe image distortions, motivated us to design a closed liquid cell for our stand-alone microscope.

Fig. 1 shows a schematic drawing of the AFM scanner with the closed liquid cell. In this set-up the sample is mounted on a steel disk, which sticks to a magnet. To reduce environmental vibrations, the bottom plate on which the sample is mounted consists of 30-mm-thick aluminum. On the mica sheet, a 5-mm inner diameter silicone o-ring is placed, on which the stand-alone AFM is mounted. The o-ring fits tightly in a groove, which is cut in a 5-mm Plexiglas top plate. The cantilever is mounted in a second groove in the top plate, which is screwed on a piezo scanner (Stavely Sensors), with a scan range of $3 \times 3\ \mu m^2$. In the top plate, two channels are drilled and sealed with a little rubber cork. Injecting liquid through a tube with an injection needle, which passes through the cork, enables exchange of buffers. To reduce image distortions caused by vibrations of the long tubes, the tubes are rigidly connected to the housing of the stand-alone AFM. A practical advantage of the stand-alone concept is that residual leakage of the liquid cell does not damage the piezo scanner, as the latter is positioned above the liquid cell. Measurements using this set-up resulted in thermal drift of the scanner of less than 100 nm/h if the o-ring was properly inserted in the groove, which was sufficient for most imaging applications.

Optimization of the bandwidth of the feedback loop

In the study of biological processes at the single molecule level, good temporal resolution is essential. In redesigning the AFM set-up, attention was paid to optimize the temporal resolution, under the condition that commercially available cantilevers should be used. For this reason, the bandwidth of the detection scheme was matched with resonance frequencies of the cantilever and the piezo. The cantilevers used for tapping mode in liquid are generally operated at 10–40 kHz, depending on acoustic modes in the liquid cell. We chose to use only the higher frequencies from 25 to 35 kHz.

Amplitude was measured, using a true root mean square (RMS) decoder, with a detection bandwidth of 5 kHz, thus averaging over only five or six oscillations. To compensate for all amplitude variations in the feedback loop, and thus minimizing tip-sample interactions, the piezo has to follow these variations with the same frequency. A tube piezo scanner with a resonance frequency of 3 kHz was chosen. A smaller piezo tube with a higher resonance frequency would better match the bandwidth of the RMS decoder, but then scan range would be sacrificed. With this configuration maximum spatial frequencies corresponding to 3 kHz can be measured, while carefully keeping the tapping amplitude constant.

Maximum scan velocity

To make full use of the bandwidth of the feedback loop, the line frequency, at which the surface is scanned, can be increased until the highest frequency of height variations in a line scan matches the feedback bandwidth. In our experiments the sharpness of the features in the AFM images, like those of proteins and DNA, is limited by the convolution with the tip. Because of this tip-sample convolution, the width of dsDNA generally broadens to 20 nm. In our experiments the fastest changes in height will occur when the tip scans perpendicular to a DNA molecule. When an area of $2 \times 2\ \mu m^2$ is scanned with a line frequency of 20 Hz, the spatial frequency of a 20-nm-wide feature, like a DNA molecule scanned perpendicular to the line scan, corresponds to 2 kHz, which is just below the bandwidth of the feedback loop. With these settings, all topography-induced amplitude changes are carefully compensated by retraction of the piezo. Thus the surface can be scanned at a maximum velocity of 20 μm/s, while the tip-sample interaction forces are kept minimal. For back traces of the tip, the same velocity is used.

For an accurate measurement of the width of tip-convolution-limited features in the images, four pixels are sampled per 20 nm, resulting in an image size of 512×512 pixels for a $2 \times 2\ \mu m^2$ scan area. The resulting typical maximum frame rate is 1 image/50 s. To improve the temporal resolution further, the scan area and frame rate can be interchanged, maintaining the same scan velocity. However, if the scan area is reduced too much, drift may cause the object to move out of the field of view.

Experiments

DNA movement over the mica surface

Fig. 2 shows three frames from a typical time series measurement of the photolyase DNA mixture. In this measurement the surface was scanned for 30 min at 1 frame/min; three frames measured at 1, 10, and 25 min are displayed. During the 30 min of scanning, no damage to the sample was visible, and RMS roughness in the height of the atomically flat mica amounted less than 0.2 nm. The drift during the measurement, as measured by cross-correlation of sequential images, amounted to 80 nm in 30 min.

For binding of photolyase to DNA, it is important that the DNA strands can come loose from the surface. The stability of the AFM and the drift correction allowed detailed comparison of the images and enable us to show that we really achieved conditions in which the DNA is only loosely attached to the surface. In Fig. 2 *d* a time average of 25 topographic images obtained over 25 min is shown. The parts of the DNA that are not attached to the surface can move during the experiment; in the resulting average height image, the DNA strands at these positions become fuzzy and have a lower intensity. Parts of the DNA that are immobile will keep the same position in the sequential images; these features appear sharp, and the intensity will equal the height of the feature in a single frame. The box drawn in Fig. 2 *c* indicates a DNA strand that is attached to the surface only at its ends. In Fig. 2 *d* the corresponding box clearly shows the two distinct sites where the DNA is fixed, and the middle part of the DNA strand that is free to move disappears in the time-averaged image. This behavior is observed for many DNA molecules in this image. The fixed DNA parts are generally separated by loose parts of DNA, which, on the average, are ~80 nm long. This may indicate that the mica surface is only partly covered with Mg^{2+} ions, which points at a stable, specific local interaction of the Mg^{2+} ions with mica. In our experiments the mobility of DNA on the surface varied a great deal when identical reaction buffers were used. Varieties in DNA binding affinity can only be attributed to nonreproducible surface properties of mica.

During the experiment a variety of molecular movements took place. One of the most striking was the opening and closing of 500-bp DNA circles. Some of these events are denoted by a circle in Fig. 2, *a–c*. In Fig. 3 the 500-bp DNA fragment in the bottom left circle is magnified and followed in time at 1 frame/min. These frames clearly show that despite the movement of the DNA molecule over the mica surface, the scanning tip can image it with a fairly good quality. Halfway through the sequence, the two ends stick together, and while the DNA molecule still has some freedom to move over the surface, the ends are tied together. The DNA fragments were cut with *Eco*RI, resulting in ends with single-stranded overhangs of four complementary bases (AATT). Breaking the hydrogen bonds between 4 bp requires a few kT (0.6 kcal/mol; Saenger, 1986), which can be provided by thermal energy. Indeed, annealing and breaking of these hydrogen bonds occurs several times in the sequence displayed in Fig. 2, as indicated by the circles. The scanning tip does not seem to disrupt hydrogen bonding between the ends, indicating minimal interference of the scanning tip with the loose molecules on the surface.

Imaging of photolyase

In Fig. 4 *a*, the white arrows indicate two photolyase molecules. The photolyase molecules appear as globular structures, which measure, on average, ~4 nm, slightly smaller than the dimensions obtained by crystallography (Tamada et

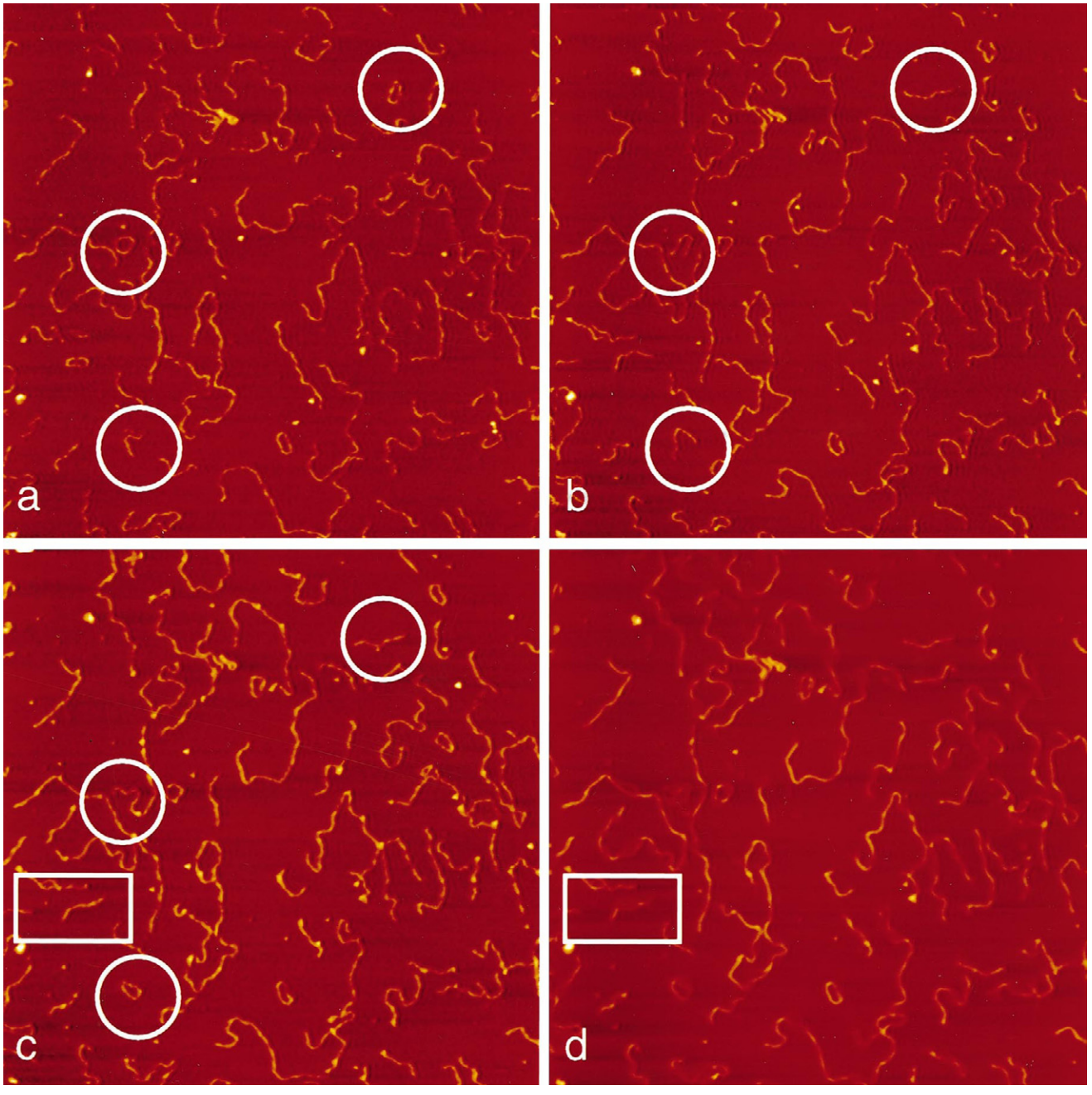

FIGURE 2 (*a–c*) Three frames from a 30-min sequence of topography images obtained by tapping mode AFM. The scan area was $2 \times 2\ \mu m^2$; *z* range, 4 nm. The frames acquired at 1 = 1, 10, and 25 min are displayed. (*d*) Time average of 25 frames of the sequence shown in *a–c*; the *z* range equals the *z* range of the single frames for easy comparison. Mobile molecules in the time-averaged image become fuzzy and less intense, whereas immobile molecules remain sharp and have the same intensity as in a single frame.

al., 1997). In AFM images, the shape of small objects like proteins is dominated by the convolution of the protein and the tip, resulting in features with a height corresponding to the height of the protein, but a lateral size that is mainly determined by the tip dimensions. Thus, on the basis of their height, the globular structures can be attributed to photolyase molecules. To confirm this, we checked that the concentration of these features on the substrate is directly related to the photolyase concentration in the buffer.

Like DNA, photolyase molecules are only loosely bound to the mica surface. Whereas the molecule indicated by the arrow on the right in Fig. 4 *a* remains at the same position during the whole experiment, pointing at a firm attachment to the surface, the molecule on the left is only loosely bound to the surface.

In Fig. 4 it can be seen that the tip can move the photolyase while it stays on the surface. During imaging, the tip scans horizontally over the surface from left to right and

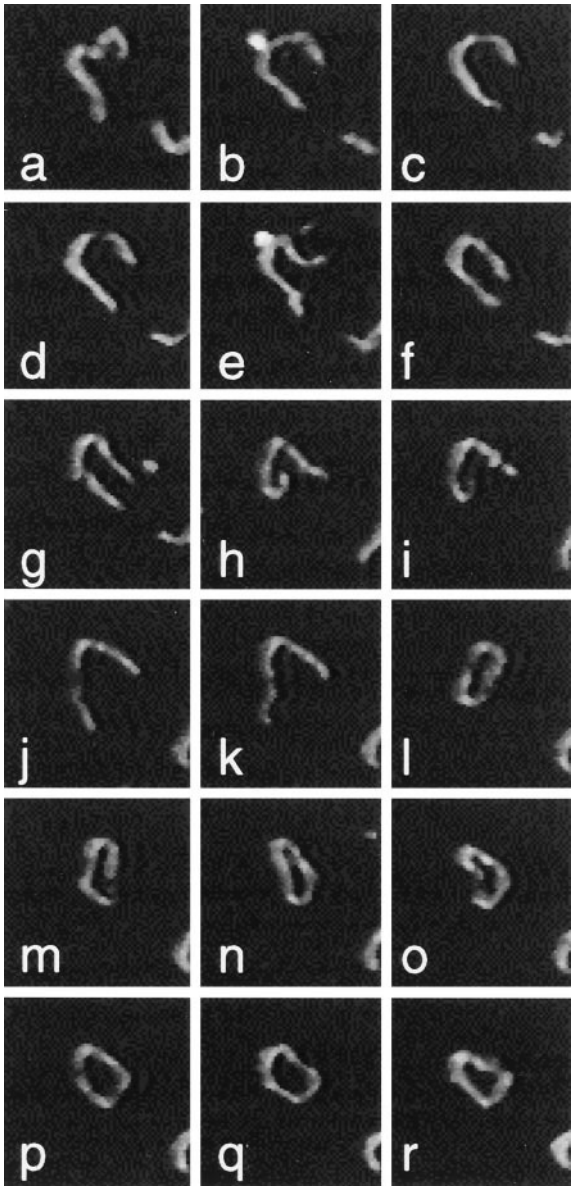

FIGURE 3 Sequence of 18 successive topography images obtained by tapping-mode AFM, showing one 500-bp DNA molecule, with an interval of 1 min. The images where cut out of the sequence displayed in Fig. 2. Scan area, 250 × 250 nm^2; z range, 4 nm.

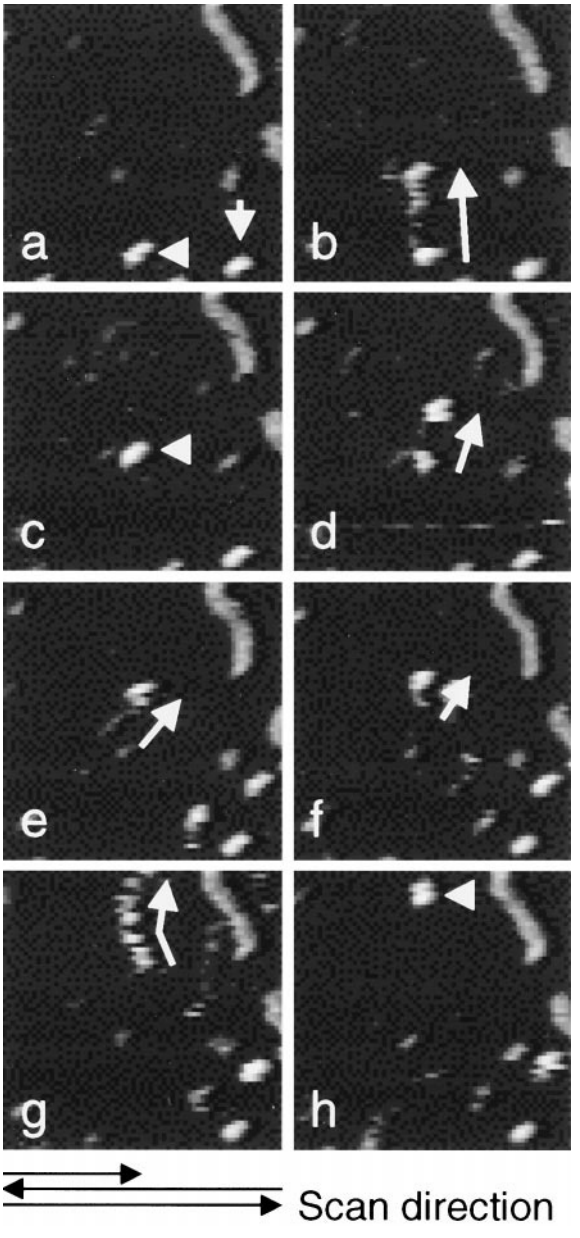

FIGURE 4 Sequence of eight successive topography images obtained by tapping-mode AFM at times t = 1, 2, 3, 4, 5, 6, 11, and 12 min. Two photolyase molecules are indicated by white arrows in *a*. White arrows in *b–h* indicate the movement of one photolyase molecule. The black arrows indicate the scan direction of the tip. Scan area, 250 × 250 nm^2; z range, 4 nm.

back, with respect to image 4. The vertical position of the line scan is slowly increased until the whole field of view is covered, as depicted schematically by the arrows below Fig. 4 *g*. The sequential images are all acquired in this way, from top to bottom. When the tip taps at the edge of the protein, the molecule moves up. In Fig. 4 *b*, the photolyase is moved up, perpendicular to the scan direction, as indicated by the white arrow. In the succeeding line scans, further upward in the image, the same molecule is detected and pushed away again, causing the bright "tail" under the molecule. In Fig. 4 *c* the protein stays at the position it was left at in the previous scan. Then in Fig. 4 *d*, either it is moved up again, or it dissolves in the solution and another molecule adsorbs to the surface. In the next figure the photolyase is only loosely attached to the surface. In the middle two lines it is moved 10 nm to the left, to move back to the right in the next scan line. Only after another six frames, 6 min later, is photolyase swept up again, to a position at which it stayed during the rest of the experiment. In Fig. 4 *e* in the bottom right corner, a new photolyase molecule adsorbs to the surface from the buffer solution. The behavior of the molecules displayed in Fig. 4 is typical for the photolyase molecules in this sequence; only directional movement upward, perpendicular to the line scan direction, is observed. The scanning tip sweeps the photolyase molecules away,

and as the tip is slowly moving upward, no downward movement of photolyase molecules is observed. Again, a large variety between experiments occurs, pointing at nonreproducible surface properties. As the photolyase covers only a few nm^2 of the surface, it is much more dependent on the local variations of the surface, and thus is more mobile than the DNA molecules. Next to the smaller contact area, the nonuniform surface charge of photolyase (Park et al., 1995) may create large differences in binding affinity for the surface, depending on the orientation of the molecule.

Photolyase-DNA interactions

In the sequence displayed in Fig. 5, the tapping tip sweeps up photolyase molecules as described in the previous section, but when a DNA strand is in the way, photolyase sticks to the DNA, forming a complex. Most complexes remain stable during the rest of the experiment, like the complex indicated by the arrow in Fig. 5 *b*. On some occasions, photolyase dissociates from the DNA, even when the complex has been stable for a few scans. In Fig. 5, *g* and *h*, photolyase in the indicated complex stays on the DNA, but appears to have moved over it. This suggests the possibility that photolyase uses a sliding mechanism to scan the DNA to find damaged sites.

In Fig. 6 another example is shown in which photolyase apparently slides over the DNA strand in the center of the image. In four frames taken directly after the formation of the complex, the position of photolyase changes by 80 nm. As the movement is downward, opposite the scan direction of the tip, it is unlikely that the tip pushed the photolyase molecule over the DNA strand. In the time span between Fig. 6 *c* and Fig. 6 *d*, the protein hardly changed position, and in the succeeding frames, which are not shown, the

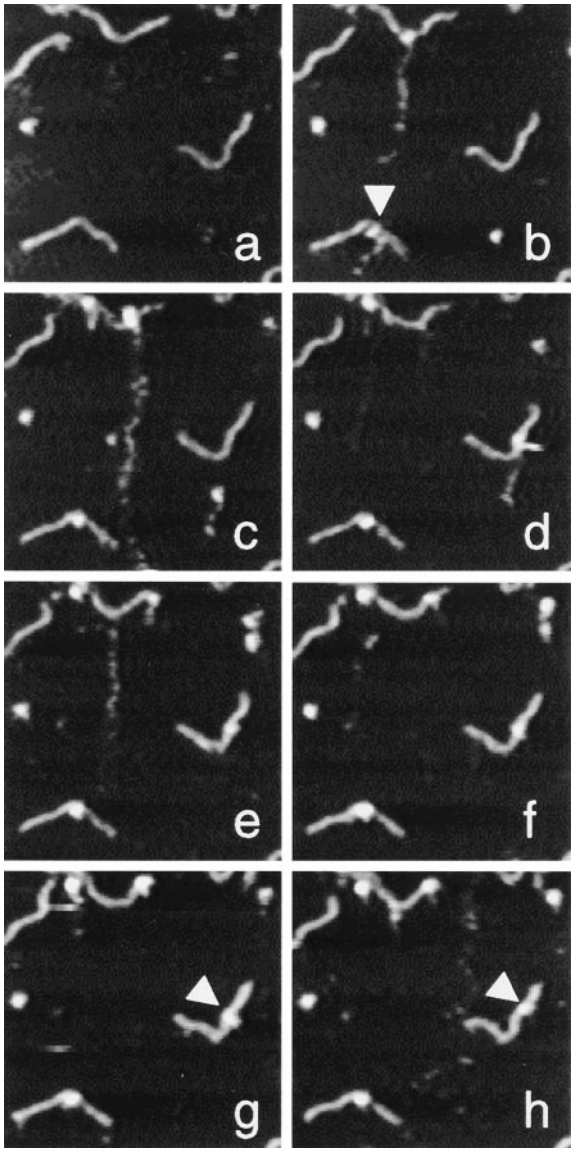

FIGURE 5 Sequence of eight topography images obtained by tapping-mode AFM, showing photolyase and DNA molecules. The arrows indicate positions where DNA and photolyase interact nonspecifically. Scan area, 500×500 nm^2; *z* range, 4 nm at times $t = 1, 4, 7, 8, 9, 10, 11$, and 12 min.

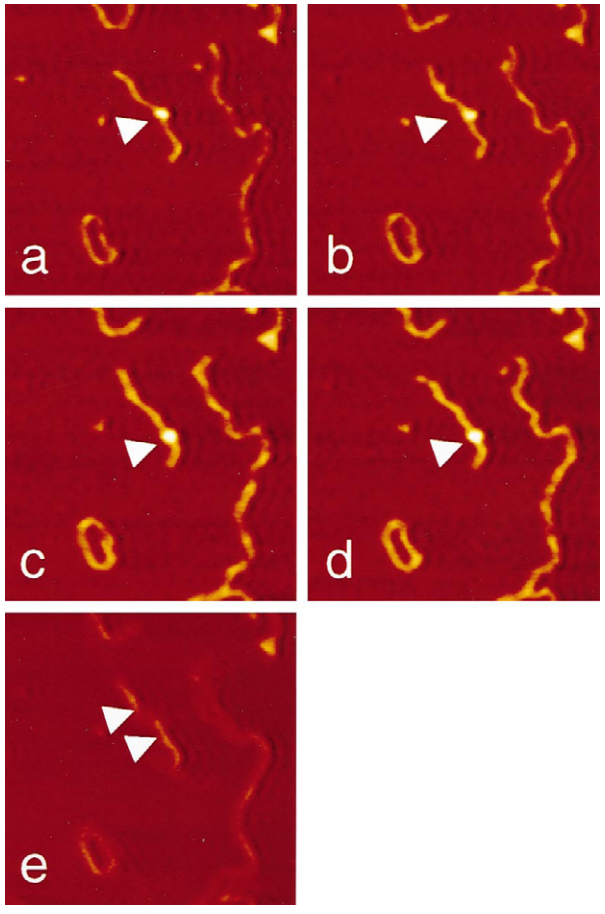

FIGURE 6 (*a–d*) Sequence of four successive topography images obtained by tapping-mode AFM with an interval of 1 min. In the figures the photolyase molecule indicated by the arrow moves over a DNA molecule. Scan area, 500×500 nm^2; *z* range, 4 nm. (*e*) Time average of 25 frames of the sequence shown in *a–d*. The *z* range equals the *z* range of the single frames for easy comparison. Mobile DNA parts become fuzzy and less intense, whereas immobile parts remain sharp and have the same intensity as in a single frame.

protein remains at the same position. The range over which the photolyase has moved agrees well with the range over which the DNA is loosely bound. In Fig. 6 *e* an average of 25 frames shows that the movement of the photolyase is confined to the range in which DNA appears fuzzier than on the boundaries of the movement, indicating that the DNA is only loosely bound in this region. Thus it is likely that the photolyase is stopped by steric hindrance at the position where DNA is firmly attached to the surface.

CONCLUSIONS AND DISCUSSION

Improvements of the AFM set-up

The modifications implemented on our AFM set-up enabled us to routinely image DNA and proteins under physiological conditions at high quality. The AFM system was optimized to keep interaction forces down to a minimum. For careful adjustment of the tapping parameters, the ability to monitor the deflection signal and to adjust the feedback parameters online appeared crucial. Thus the feedback loop could be kept stable very accurately for more than half an hour, resulting in no recognizable damage and background RMS noise of less than 0.2 nm. Even loose molecules can be imaged with the tip, although sometimes very mobile photolyase proteins were swept away.

Assuming that the amplitude of the free cantilever's movement decreases linearly when it approaches the surface, the peak force the tip exerts on the sample can be estimated (Putman et al., 1994). For this estimation it is assumed that all amplitude variations are carefully compensated for by the feedback loop. Under the conditions used in our experiments, the maximum force exerted on the surface when the tip touches the surface for only a few microseconds is estimated to be a few hundred piconewtons. Thus the repulsive forces balance the attractive adhesion forces between the tip and the sample. Further reduction of interaction forces would not only require smaller tapping amplitudes, lower damping, or weaker spring constants; tip adhesion would have to be reduced as well. One way to fulfill this requirement is to use electron beam-deposited supertips. These supertips decrease tip-sample adhesion, as the tip-sample contact area is smaller. Thus smaller tapping amplitudes may be used, which would further decrease interaction forces. In addition to this effect, the spatial resolution of the measurements would further improve, although the spatial resolution of the reported measurements is sufficient to easily identify single proteins and DNA strands.

Recently, direct magnetic excitation of the cantilever was introduced (Han and Lindsay, 1996). Direct excitation of the cantilever minimizes acoustic vibrations in the liquid, which, compared to acoustic excitation, may better stabilize the loosely bound molecules on the surface. Promising results have been reported, indicating a gentler way to scan the surface (Han and Lindsay, 1997). Although we have shown that good results can be obtained using acoustic excitation when all parameters are carefully optimized, this new way of excitation may improve the image quality even further.

The scan rate of our system was maximized for commercially available cantilevers to 20 μm/s. For the experiments reported in this article, this was sufficient to distinguish between different positions of the DNA on the surface, and even the dynamics of nonspecific DNA-protein interactions could be observed. As for most of our analysis, only part of the image was used, and thus the scan area could be decreased to increase the frame rate, keeping the scan velocity constant. As the frame rate is inversely proportional to the scan area, the scan area could be sacrificed as much as the drift allowed. However, because of the variations in behavior of the individual molecules, a better representation of the processes between these molecules is obtained when more of these molecules are followed simultaneously. This is especially important, because the surface properties of the mica vary between experiments, which make quantitative comparisons between different experiments difficult.

To increase the scan rate without sacrificing the field of view, a number of improvements need to be made. First cantilevers with a higher resonance frequency must be made (Walters et al., 1996). To limit sample damage, it is necessary to keep the spring constant as small as possible. Furthermore, a piezo with higher resonance frequency should be used, to accurately compensate for all amplitude variations with the feedback loop.

Immobilization of DNA

In this paper we have shown that DNA is very inhomogeneously bound to the mica substrate in a buffer containing 1 mM NaCl and 1 mM $MgCl_2$. The data presented here are all from experiments in which DNA was bound loosely to the surface. In some experiments not presented in this paper, the DNA did not move at all during the 30 min of image acquisition. The natural diversity of mica may explain the large variation in the binding of DNA.

It is very likely that the presence of the surface slowed down the movements of the molecules. Guthold et al. (manuscript submitted for publication) measured a two-dimensional diffusion constant of 25 nm^2/s for 1000-bp DNA fragments over a mica surface under similar imaging conditions, although the ability of the DNA to diffuse over the surface depended strongly on the DNA-mica adsorption and the resulting friction. The data presented in this study show very inhomogeneous, localized absorption of DNA to mica. Thus the model of free two-dimensional diffusion of DNA over the surface, which implies a homogeneously distributed potential well for DNA adsorption on the surface, does not apply for our measurements.

In the case of loosely bound DNA, time averaging of a series of images reveals sites on the mica where the DNA is tightly bound, and other parts that are not bound to the surface. This nicely reveals the very local interaction re-

sponsible for immobilising DNA. Hansma and Laney (1996) showed that K^+ ions at the mica surface are exchanged with Mg^{2+} from the buffer. This interpretation suggests that only some of the K^+ ions are replaced when the buffer contains 1 mM NaCl and 1 mM $MgCl_2$.

DNA-photolyase interactions

We used AFM to visualize dynamic interactions between photolyase and DNA. As the DNA was undamaged, we do not address actual damage recognition with these experiments, but we studied the previous step of locating these sites. We did observe photolyase moving over loose pieces of the DNA, suggesting that photolyase uses one-dimensional diffusion to scan the DNA for damaged sites. Points of firm DNA attachment appeared to stop photolyase movement. Thus the presence of the surface will have a great influence on the observed rate and extent of sliding.

In the experiments in which no movement of DNA was observed (not shown), photolyase did not move over the DNA. This did not prevent photolyase from association and dissociation with undamaged DNA fragments. Photolyase has only a low affinity ($K_d = 10^{-4}$ M) for undamaged double-stranded DNA (Park et al., 1995). Any one-dimensional diffusion on the DNA has to compete with dissociation of the complex. Furthermore, as no energy source is available for the proposed sliding of the photolyase on the DNA, friction or steric hindrance would be expected to prevent the protein from sliding over the DNA.

Competition with dissociation of the complex reduces the effective range over which the photolyase might slide. Indeed, the average range through which other proteins (like T4-endonuclease V) scan over DNA is dependent on the ionic strength of the buffer, which strongly affects the binding affinity of this protein (Dowd and Lloyd, 1990). In this study relatively low ion concentrations were used, to favor possible sliding of photolyase over DNA.

Like the movement of photolyase over the surface, the scanning tip may induce movement of photolyase over DNA. However, as sliding of photolyase over DNA was observed in all directions relative to the scanning tip, it seems unlikely that effects of the scanning tip dominate the movement of photolyase along DNA. Another observation, which points at a one-dimensional diffusion of photolyase over DNA, is that the mobility is limited to loose parts of the DNA. As no energy is available for the motion, DNA cannot be actively pulled from the surface by the protein. Future studies will have to establish whether photolyase indeed slides along the DNA. In this paper we have shown that, when all measurement parameters are carefully optimized, AFM measurements under physiological conditions provide a tool for investigating the dynamics of molecular interaction mechanisms between DNA and proteins on a single-molecule scale.

This work was supported by the Dutch Organisation for Fundamental Research on Matter (FOM) (grant 94BR1231).

REFERENCES

Berg, O., R. B. Winter, and P. H. von Hippel. 1981. Diffusion-driven mechanism of protein translocation on nucleic acids. 1. Models and theory. *Biochemistry.* 20:6929–6948.

Butt, H.-J., and M. Jaschke. 1995. Calculation of thermal noise in atomic force microscopy. *Nanotechnology.* 6:1–7.

Dowd, D. R., and R. S. Lloyd. 1990. Biological significance of facilitated diffusion in protein-DNA interactions. *J. Biol. Chem.* 265:3424–3431.

Eker, A. P. M., P. Kooiman, J. K. C. Hessels, and A. Yasui. 1990. DNA photoreactivating enzyme from the cyanobacterium *Anacystis nidulans*. *J. Biol. Chem.* 265:8009–815.

Erie, D. A., G. Yang, H. C. Schultz, and C. Bustamante. 1994. DNA bending by Cro protein in specific and nonspecific complexes: implications for protein site recognition and specifity. *Science.* 266:1562–1566.

Florin, E.-L., V. T. Moy, and H. E. Gaub. 1994. Intermolecular forces and energies between ligands and receptors. *Science.* 266:257–259.

Guthold, M., M. Bezanilla, D. A. Erie, B. Jenkins, H. G. Hansma, and C. Bustamante. 1994. Following the assembly of RNA polymerase-DNA complexes in aqueous solutions with the scanning force microscope. *Proc. Natl. Acad. Sci. USA.* 91:12927–12931.

Han, W., and S. M. Lindsay. 1996. A magnetically driven oscillating probe microscope for operations in liquids. *Appl. Phys. Lett.* 69:4111–4113.

Han, W., and S. M. Lindsay. 1997. Kinked DNA. *Nature.* 386:563.

Hansma, H. G. 1995. Atomic force microscopy of biomolecules. *J. Vac. Sci. Technol. B.* 14:1390–1395.

Hansma, H. G., and D. E. Laney. 1996. DNA binding correlates with cationic radius: assay by atomic force microscopy. *Biophys. J.* 70: 1933–1939.

Hansma, P. K., J. P. Cleveland, M. Radmacher, D. A. Walters, and P. Hillner. 1994. Tapping mode atomic force microscopy in liquids. *Appl. Phys. Lett.* 64:1738–1740.

Hansma, H. G., I. Revenko, K. Kim, and D. E. Laney. 1996. Atomic force microscopy of long and short double-stranded, single-stranded and triple-stranded nucleic acids. *Nucleic Acids Res.* 24:713–720.

Hearst, J. E. 1995. The structure of photolyase: using photon energy for DNA repair. *Science.* 268:1858–1868.

Kasas, S., N. H. Thomson, B. L. Smith, H. G. Hansma, X. Zhu, M. Guthold, C. Bustamante, E. T. Kool, M. Kashev, and P. K. Hansma. 1997. *Escherichia coli* RNA polymerase activity observed using atomic force microscopy. *Biochemistry.* 36:461–468.

Lal, R., and S. A. John, 1994. Biological applications of atomic force microscopy. *Am. J. Physiol.* 266:1–21.

Park, H.-W., S.-T. Kim, A. Sancar, and J. Deisenhofer. 1995. Crystal structure of DNA photolyase from *Escherichia coli*. *Science.* 268: 1866–1872.

Putman, C. A., K. O. van der Werf, B. G. de Grooth, N. F. van Hulst, and J. Greve. 1994. Tapping mode atomic force microscopy in liquid. *Appl. Phys. Lett.* 64:2454–2456.

Radmacher, M., M. Fritz, H. G. Hansma, and P. K. Hansma. 1994. Direct observation of enzyme activity with the atomic force microscope. *Science.* 265:1577–1579.

Saenger, W. 1986. Principles of Nucleic Acid Structure. Springer Verlag, New York.

Sancar, A. 1994. Structure and function of DNA photolyase. *Biochemistry.* 33:2–9.

Schäfer, T. E., J. P. Cleveland, F. Ohnesorge, D. A. Walters, and P. K. Hansma. 1996. Studies of vibrating atomic cantilevers in liquid. *J. Appl. Phys.* 80:3622–3627.

Tamada, T., K. Kitadoro, Y. Higuchi, K. Inaka, A. Yasui, P. E. de Ruiter, A. P. M. Eker, and K. Miki. 1997. Crystal structure of DNA photolyase from *Anacystus nidulans*. *Nature Struct. Biol.* 4:887–891.

Thomson, N. H., S. Kasas, B. Smith, H. G. Hansma, and P. K. Hansma. 1996. Reversible binding of DNA to mica for AFM imaging. *Langmuir.* 12:5905–5908.

Van der Werf, K. O., C. A. Putman, B. G. de Grooth, F. B. Segerink, E. H. Schipper, N. F. van Hulst, and J. Greve. 1993. Compact stand-alone atomic force microscope. *Rev. Sci. Instrum.* 64:2892–2897.

Van Noort, S. J. T., K. O. van der Werf, B. G. de Grooth, N. F. van Hulst, and J. Greve. 1997. Height anomalies in tapping mode atomic force microscopy in air caused by adhesion. *Ultramicroscopy.* 69:117–127.

Walters, D. A., J. P. Cleveland, N. H. Thomson, and P. K. Hansma. 1996. Short cantilevers for atomic force microscopy. *Rev. Sci. Instrum.* 67: 3583–3590.

Wyman, C., E. Grottkopp, C. Bustamante, and H. C. M. Nelson. 1995. Determination of heat-shock transcription factor 2 stoichiometry at looped DNA complexes using scanning force microscopy. *EMBO J.* 14:117–123.

Wyman, C., I. Rombel, A. K. North, C. Bustamante, and S. Kustu. 1997. Unusual oligomerisation required for activity of NtrC, a bacterial enhancer-binding protein. *Science.* 275:1658–1661.